Observation of the $\psi(4415) \to D\bar{D}_2^*(2460)$ Decay Using Initial-State Radiation

G. Pakhlova,[11] I. Adachi,[6] H. Aihara,[41] K. Arinstein,[1] V. Aulchenko,[1] T. Aushev,[16,11] A. M. Bakich,[36] V. Balagura,[11] E. Barberio,[19] I. Bedny,[1] K. Belous,[10] U. Bitenc,[12] A. Bondar,[1] M. Bračko,[18,12] J. Brodzicka,[6] T. E. Browder,[5] A. Chen,[21] W. T. Chen,[21] B. G. Cheon,[4] C.-C. Chiang,[23] R. Chistov,[11] I.-S. Cho,[46] Y. Choi,[35] J. Dalseno,[19] M. Danilov,[11] M. Dash,[45] A. Drutskoy,[2] S. Eidelman,[1] D. Epifanov,[1] N. Gabyshev,[1] B. Golob,[17,12] H. Ha,[14] J. Haba,[6] K. Hayasaka,[20] M. Hazumi,[6] D. Heffernan,[29] Y. Hoshi,[39] W.-S. Hou,[23] Y. B. Hsiung,[23] H. J. Hyun,[15] K. Inami,[20] A. Ishikawa,[32] H. Ishino,[42] R. Itoh,[6] M. Iwasaki,[41] Y. Iwasaki,[6] N. J. Joshi,[37] D. H. Kah,[15] J. H. Kang,[46] T. Kawasaki,[26] A. Kibayashi,[6] H. Kichimi,[6] H. J. Kim,[15] H. O. Kim,[35] Y. J. Kim,[3] K. Kinoshita,[2] S. Korpar,[18,12] P. Križan,[17,12] P. Krokovny,[6] R. Kumar,[30] C. C. Kuo,[21] A. Kuzmin,[1] Y.-J. Kwon,[46] J. S. Lange,[47] M. J. Lee,[34] S. E. Lee,[34] T. Lesiak,[24] S.-W. Lin,[23] D. Liventsev,[11] F. Mandl,[9] D. Marlow,[31] S. McOnie,[36] T. Medvedeva,[11] H. Miyake,[29] R. Mizuk,[11] D. Mohapatra,[45] G. R. Moloney,[19] Y. Nagasaka,[7] E. Nakano,[28] M. Nakao,[6] H. Nakazawa,[21] S. Nishida,[6] O. Nitoh,[44] S. Ogawa,[38] T. Ohshima,[20] S. Okuno,[13] S. L. Olsen,[5,8] H. Ozaki,[6] P. Pakhlov,[11] H. Park,[15] K. S. Park,[35] L. S. Peak,[36] R. Pestotnik,[12] L. E. Piilonen,[45] A. Poluektov,[1] Y. Sakai,[6] O. Schneider,[16] C. Schwanda,[9] K. Senyo,[20] M. Shapkin,[10] C. P. Shen,[8] H. Shibuya,[38] J.-G. Shiu,[23] B. Shwartz,[1] J. B. Singh,[30] A. Somov,[2] S. Stanič,[27] T. Sumiyoshi,[43] F. Takasaki,[6] K. Tamai,[6] M. Tanaka,[6] G. N. Taylor,[19] Y. Teramoto,[28] I. Tikhomirov,[11] S. Uehara,[6] K. Ueno,[23] T. Uglov,[11] Y. Unno,[4] S. Uno,[6] Y. Usov,[1] G. Varner,[5] A. Vinokurova,[1] C. H. Wang,[22] M.-Z. Wang,[23] P. Wang,[8] X. L. Wang,[8] Y. Watanabe,[13] E. Won,[14] B. D. Yabsley,[36] A. Yamaguchi,[40] Y. Yamashita,[25] M. Yamauchi,[6] C. Z. Yuan,[8] C. C. Zhang,[8] L. M. Zhang,[33] Z. P. Zhang,[33] V. Zhilich,[1] V. Zhulanov,[1] and A. Zupanc[12]

(Belle Collaboration)

[1]*Budker Institute of Nuclear Physics, Novosibirsk*
[2]*University of Cincinnati, Cincinnati, Ohio 45221*
[3]*The Graduate University for Advanced Studies, Hayama*
[4]*Hanyang University, Seoul*
[5]*University of Hawaii, Honolulu, Hawaii 96822*
[6]*High Energy Accelerator Research Organization (KEK), Tsukuba*
[7]*Hiroshima Institute of Technology, Hiroshima*
[8]*Institute of High Energy Physics, Chinese Academy of Sciences, Beijing*
[9]*Institute of High Energy Physics, Vienna*
[10]*Institute of High Energy Physics, Protvino*
[11]*Institute for Theoretical and Experimental Physics, Moscow*
[12]*J. Stefan Institute, Ljubljana*
[13]*Kanagawa University, Yokohama*
[14]*Korea University, Seoul*
[15]*Kyungpook National University, Taegu*
[16]*École Polytechnique Fédérale de Lausanne (EPFL), Lausanne*
[17]*University of Ljubljana, Ljubljana*
[18]*University of Maribor, Maribor*
[19]*University of Melbourne, School of Physics, Victoria 3010*
[20]*Nagoya University, Nagoya*
[21]*National Central University, Chung-li*
[22]*National United University, Miao Li*
[23]*Department of Physics, National Taiwan University, Taipei*
[24]*H. Niewodniczanski Institute of Nuclear Physics, Krakow*
[25]*Nippon Dental University, Niigata*
[26]*Niigata University, Niigata*
[27]*University of Nova Gorica, Nova Gorica*
[28]*Osaka City University, Osaka*
[29]*Osaka University, Osaka*
[30]*Panjab University, Chandigarh*
[31]*Princeton University, Princeton, New Jersey 08544*
[32]*Saga University, Saga*
[33]*University of Science and Technology of China, Hefei*
[34]*Seoul National University, Seoul*

 © 2008 The American Physical Society

[35]Sungkyunkwan University, Suwon
[36]University of Sydney, Sydney, New South Wales
[37]Tata Institute of Fundamental Research, Mumbai
[38]Toho University, Funabashi
[39]Tohoku Gakuin University, Tagajo
[40]Tohoku University, Sendai
[41]Department of Physics, University of Tokyo, Tokyo
[42]Tokyo Institute of Technology, Tokyo
[43]Tokyo Metropolitan University, Tokyo
[44]Tokyo University of Agriculture and Technology, Tokyo
[45]Virginia Polytechnic Institute and State University, Blacksburg, Virginia 24061
[46]Yonsei University, Seoul
[47]Justus-Liebig-Universität Gießen, Gießen

(Received 24 August 2007; published 13 February 2008)

We report measurements of the exclusive cross section for $e^+e^- \to D^0D^-\pi^+$ over the center-of-mass energy range 4.0 GeV to 5.0 GeV with initial-state radiation and the first observation of the decay $\psi(4415) \to D^0D^-\pi^+$. From a study of the resonant substructure in $\psi(4415)$ decay we conclude that the $\psi(4415) \to D^0D^-\pi^+$ decay is dominated by $\psi(4415) \to D\bar{D}_2^*(2460)$. We obtain $\mathcal{B}(\psi(4415) \to D^0D^-\pi^+_{\rm nonresonant})/\mathcal{B}(\psi(4415) \to D\bar{D}_2^*(2460) \to D^0D^-\pi^+) < 0.22$ at 90% C.L. The analysis is based on a data sample collected with the Belle detector with an integrated luminosity of 673 fb^{-1}.

DOI: 10.1103/PhysRevLett.100.062001 PACS numbers: 13.66.Bc, 13.87.Fh, 14.40.Gx

The $\psi(4415)$ resonance, the heaviest well-established $J^{PC} = 1^{--}$ charmonium state, was first observed 30 years ago by the Mark I [1] and DASP [2] collaborations. Subsequently, although additional e^+e^- annihilation cross section measurements in the region of the $\psi(4415)$ were reported by the Crystal Ball [3] and BESII [4] groups, no update of its parameters was done until 2005, when a combined fit to Crystal Ball and BESII data was performed by Seth [5]. Recently, the BES Collaboration [4] reported new parameter values for the $\psi(3770)$, $\psi(4040)$, $\psi(4160)$, and $\psi(4415)$ resonances that are derived from a global fit to their cross section measurements.

Despite the kinematic accessibility of ten open-charm strong decay modes for the $\psi(4415)$, its decays to any exclusive final states were not measured until last year, when a study of exclusive $e^+e^- \to D\bar{D}$ production via initial-state radiation (ISR) at Belle [6] revealed a small enhancement near the $\psi(4415)$ mass. A similar study [7] of $D\bar{D}^*$ production has no evident $\psi(4415)$ signal; the $D^*\bar{D}^*$ channel exhibits a small enhancement that may be attributable to the $\psi(4415)$, albeit at a slightly shifted mass value.

In this Letter we report a measurement of the exclusive cross section for the process $e^+e^- \to D^0D^-\pi^+$ and the first observation of $\psi(4415) \to D\bar{D}_2^*(2460)$ decay. It represents a continuation of our studies of the exclusive open-charm production in the mass range where recently several new charmoniumlike states were observed [$Y(4260)$ [8,9], $Y(4360)$, $Y(4660)$ [10], $X(4160)$ [11]] decaying to either open- or closed-charm final states. Our study provides further information on the dynamics of charm quarks at these center-of-mass energies and on the properties of the $\psi(4415)$. The data sample corresponds to an integrated luminosity of 673 fb^{-1} collected with the Belle detector [12] at the $\Upsilon(4S)$ resonance and nearby continuum at the KEKB asymmetric-energy e^+e^- collider [13].

We select $e^+e^- \to D^0D^-\pi^+\gamma_{\rm ISR}$ signal candidates in which the D^0, D^-, and π^+ mesons are fully reconstructed [14]. In general, the $\gamma_{\rm ISR}$ is not required to be detected and its presence in the event is inferred from a peak at zero in the spectrum of masses recoiling against the $D^0D^-\pi^+$ system. The recoil mass squared is defined as: $M^2_{\rm rec}(DD\pi) = (E_{\rm c.m.} - E_{DD\pi})^2 - p^2_{DD\pi}$. Here $E_{\rm c.m.}$ is the initial e^+e^- center-of-mass (c.m.) energy; $E_{DD\pi}$ and $p_{DD\pi}$ are the c.m. energy and momentum of the $D^0D^-\pi^+$ system, respectively. To suppress background two cases are considered: (1) the $\gamma_{\rm ISR}$ is out of detector acceptance in which case the polar angle for the $D^0D^-\pi^+$ system is required to satisfy $|\cos(\theta_{D^0D^-\pi^+})| > 0.9$; (2) the fast $\gamma_{\rm ISR}$ is within the detector acceptance ($|\cos(\theta_{D^0D^-\pi^+})| < 0.9$); in the latter case the $\gamma_{\rm ISR}$ is required to be detected with the mass of the $D^0D^-\pi^+\gamma_{\rm ISR}$ system greater than $E_{\rm c.m.} - 0.58$ GeV/c^2. To suppress backgrounds from $e^+e^- \to D\bar{D}n\pi\gamma_{\rm ISR}$ ($n > 1$) processes, we exclude events that contain additional charged tracks that are not used in D^0, D^-, or π^+ reconstruction.

All charged tracks are required to originate from the vicinity of the interaction point (IP); we impose the requirements $dr < 2$ cm and $|dz| < 4$ cm, where dr and $|dz|$ are the impact parameters perpendicular to and along the beam direction with respect to the IP. Charged kaons are required to have a ratio of particle identification likelihoods, $\mathcal{P}_K = \mathcal{L}_K/(\mathcal{L}_K + \mathcal{L}_\pi)$ [15], larger than 0.6. No identification requirements are applied for pion candidates. K^0_S candidates are reconstructed from $\pi^+\pi^-$ pairs with an invariant mass within 10 MeV/c^2 of the nominal K^0_S mass. The distance between the two pion tracks at the K^0_S vertex must be less than 1 cm, the transverse flight distance from

the interaction point is required to be greater than 0.1 cm, and the angle between the K^0_S momentum direction and the flight direction in the x-y plane should be smaller than 0.1 rad. Photons are reconstructed in the electromagnetic calorimeter as showers with energies greater than 50 MeV that are not associated with charged tracks. Pairs of photons are combined to form π^0 candidates. If the mass of a $\gamma\gamma$ pair lies within 15 MeV/c^2 of the nominal π^0 mass, the pair is fit with a π^0 mass constraint and considered as a π^0 candidate. D^0 candidates are reconstructed using five decay modes: $K^-\pi^+$, K^-K^+, $K^-\pi^-\pi^+\pi^+$, $K^0_S\pi^+\pi^-$, and $K^-\pi^+\pi^0$. A ± 15 MeV/c^2 mass window is used for all modes except for $K^-\pi^-\pi^+\pi^+$, where a ± 10 MeV/c^2 requirement is applied ($\sim 2.5\sigma$ in each case). D^+ candidates are reconstructed using the decay modes $K^0_S\pi^+$ and $K^-\pi^+\pi^+$. A ± 15 MeV/c^2 mass window is used for all D^+ modes. To improve the momentum resolution of D meson candidates, final tracks are fitted to a common vertex with a mass constraint on the nominal D^0 or D^+ mass. Candidates in the D sideband region are selected for the background study and refitted to the central mass value of either side of the sideband that has the same width as the signal window. To remove contributions from $e^+e^- \to D^-D^{*+}\gamma_{\rm ISR}$, $D^0\pi^+$ combinations with invariant mass within ± 10 MeV/c^2 of the nominal D^{*+} mass are vetoed.

The distribution of $M^2_{\rm rec}(D^0D^-\pi^+)$ for the signal region is shown in Fig. 1(a). A clear peak corresponding to the process $e^+e^- \to D^0D^-\pi^+\gamma_{\rm ISR}$ is evident around zero. The shoulder at higher masses is due to $e^+e^- \to D^0D^-\pi^+(n)\pi^0\gamma_{\rm ISR}$ events, which include $D^{*0(-)} \to D^{0(-)}\pi^0$ decays. To suppress the tail of such events we define the $M^2_{\rm rec}(D^0D^-\pi^+)$ signal region by a tight requirement ± 0.7 (GeV/c^2)^2 around zero. The polar angle distributions of $D^0D^-\pi^+$ and the mass spectrum of the $D^0D^-\pi^+\gamma_{\rm ISR}$ combinations (when $\gamma_{\rm ISR}$ is detected) in the data shown in Fig. 1(b) and 1(c), respectively, are typical of ISR production and agree with the Monte Carlo (MC) simulation. The $M_{D^0D^-\pi^+}$ spectrum after the application of all requirements is shown in Fig. 1(d). A clear peak is evident around the $\psi(4415)$ mass.

The following sources of background are considered: (1) combinatorial background under the $D^0(D^-)$ peak combined with a real $D^-(D^0)$ coming from the signal or other processes; (2) both D^0 and D^- candidates are combinatorial; (3) reflection from the processes $e^+e^- \to D^0D^-\pi^+\pi^0_{\rm miss}\gamma_{\rm ISR}$, with an extra $\pi^0_{\rm miss}$ in the final state, including $D^{*0(-)} \to D^{0(-)}\pi^0_{\rm miss}$ decays; (4) reflection from the process $e^+e^- \to D^{*0}D^-\pi^+\gamma_{\rm ISR}$, followed by $D^{*0} \to D^0\gamma$, with an extra soft γ in the final state; (5) $e^+e^- \to D^0D^-\pi^+\pi^0$ in which an energetic π^0 is misidentified as a single $\gamma_{\rm ISR}$. The contribution of background (1) is extracted using M_{D^0} and M_{D^-} sidebands that are 4 times as large as the signal region. These sidebands are shifted by 30 MeV/c^2 (20 MeV/c^2 for the $D^0 \to K^-\pi^-\pi^+\pi^+$ mode) from the signal region to avoid signal oversubtraction. Background (2) is present in both the M_{D^0} and M_{D^-} sidebands and is, thus, subtracted twice. To account for this oversubtraction we use a two-dimensional sideband region, where events are selected from both the M_{D^0} and the M_{D^-} sidebands. Backgrounds (1)–(2), ~15% of the signal, are subtracted from the signal-region $D^0D^-\pi^+$ mass spectrum. The dominant component of backgrounds (3)–(4) is suppressed by the tight requirement on $M^2_{\rm rec}(D^0D^-\pi^+)$. The remaining background from (3) is estimated by applying a similar full reconstruction method to the isospin-conjugated processes $e^+e^- \to D^0\bar{D}^0\pi^+\pi^-_{\rm miss}\gamma_{\rm ISR}$ and $e^+e^- \to D^+D^-\pi^+\pi^-_{\rm miss}\gamma_{\rm ISR}$. Here the absence of additional charged tracks in the event is not required. Because of the charge imbalance in the $D^0\bar{D}^0\pi^+$ and $D^+D^-\pi^+$ final states, only events with a

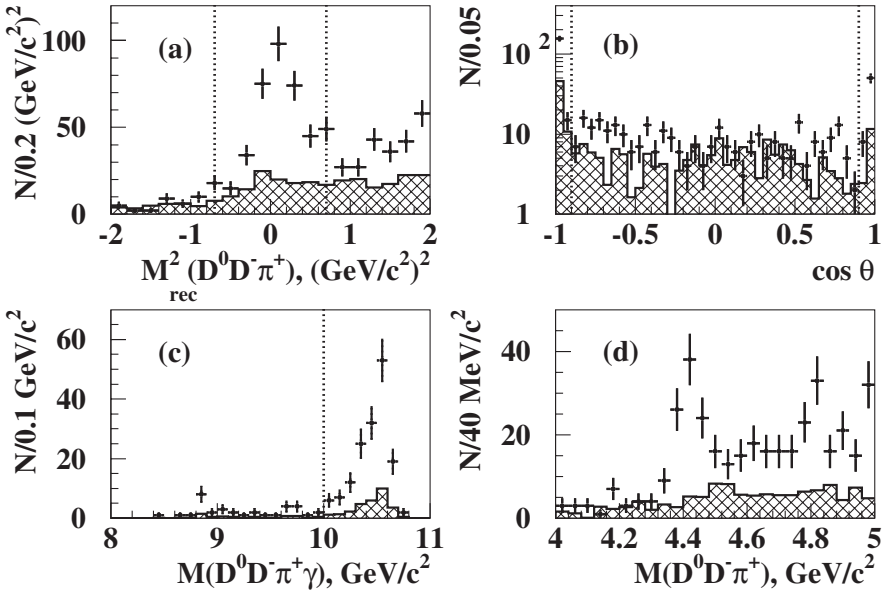

FIG. 1. The observed distributions of (a) $M^2_{\rm rec}(D^0D^-\pi^+)$ and (b) $D^0D^-\pi^+$ polar angles. (c) The $D^0D^-\pi^+\gamma_{ISR}$ mass spectrum. (d) The resulting $M_{D^0D^-\pi^+}$ spectrum. Histograms show the normalized contributions from the M_{D^0} and M_{D^-} sidebands. The selected signal windows are indicated by vertical lines.

missing extra $\pi^-_{\rm miss}$ can contribute to the $M^2_{\rm rec}(D^0\bar{D}^0\pi^+)$ and $M^2_{\rm rec}(D^+D^-\pi^+)$ signal windows. To extract the level of background (3), the $D^0\bar{D}^0\pi^+$ and $D^+D^-\pi^+$ mass spectra are rescaled according to the ratio of D^- and D^0 reconstruction efficiencies and a factor of $1/2$ due to isospin. The averaged rescaled $D^0\bar{D}^0\pi^+$ and $D^+D^-\pi^+$ mass spectrum, which is small ($\sim$2% of the signal), is subtracted from the signal-region $M_{D^0D^-\pi^+}$ spectrum. Background (4) is also estimated from the data assuming isospin symmetry. We measure the process $e^+e^- \to D^{*-}D^0\pi^+\gamma_{\rm ISR}$ ($D^{*-} \to \bar{D}^0\pi^-$) applying a similar full reconstruction method. The shape and normalization of this spectrum after efficiency correction is then used to generate a MC sample of $e^+e^- \to D^{*0}D^-\pi^+\gamma_{\rm ISR}$ ($D^{*0} \to D^0\gamma$) events. From this MC sample, tuned to the data, the contribution from background (4) is estimated to be less than $\sim$1.5 events/bin, which is subtracted from the signal $M_{D^0D^-\pi^+}$ spectrum. The contribution from background (5) is determined from reconstructed $e^+e^- \to D^0D^-\pi^+\pi^0$ events in the data found to be negligibly small and taken into account in the systematic error.

The $e^+e^- \to D^0D^-\pi^+$ cross section is extracted from the background-subtracted $D^0D^-\pi^+$ mass distribution following the procedure described in [7], taking into account the differential ISR luminosity and the total efficiency, which is found to have linear dependence on $M_{D^0D^-\pi^+}$. The resulting $e^+e^- \to D^0D^-\pi^+$ exclusive cross section is shown in Fig. 2. Since the bin width is much larger than resolution, no correction for resolution is applied.

The systematic errors for the $\sigma(e^+e^- \to D^0D^-\pi^+)$ measurements are summarized in Table I. The systematic errors associated with the background (1)–(2) subtraction are estimated to be 2% due to an uncertainty in the scaling factors for the sideband subtractions. It is estimated using fits to the M_{D^0} and M_{D^-} distributions in the data with different signal and background parametrization. Backgrounds (3)–(5) are also subtracted using the data and only the uncertainty in the scaling factors for the subtracted distribution is taken into account. Uncertainties in backgrounds (3)–(5) are estimated conservatively to be smaller than 4.5% of the signal. The systematic error ascribed to the cross section calculation includes a 1.5% error on the differential luminosity and 4.5% error in the total efficiency fit. Another source of systematic error comes from uncertainties in track and photon reconstruction efficiencies (1% per track and 1.5% per photon). Other contributions come from the uncertainty in the kaon identification efficiency and the absolute D^0 and D^- branching fractions [16].

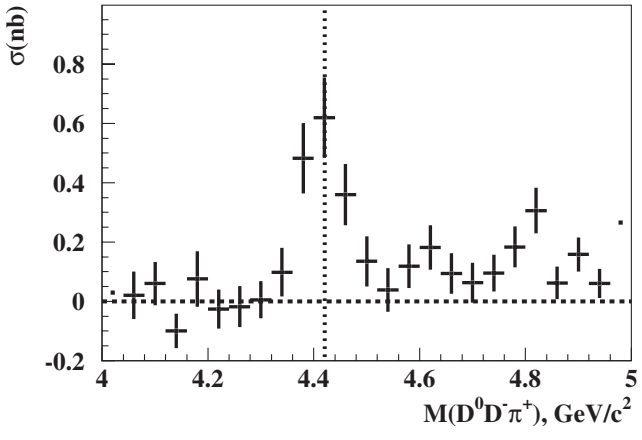

FIG. 2. The exclusive cross section for $e^+e^- \to D^0D^-\pi^+$. The dotted line corresponds to the nominal mass of the $\psi(4415)$ [16].

To study the resonant structure in $\psi(4415)$ decays, we select $D^0D^-\pi^+$ combinations from a ± 100 MeV/c^2 mass window around the nominal $\psi(4415)$ mass ($m_{\psi(4415)} = 4.421$ GeV/c^2 [16]). A scatter plot of $M(D^-\pi^+)$ versus $M(D^0\pi^+)$ and its projections onto both axes are shown in Figs. 3(a)–3(c), respectively. Clear signals for the $\bar{D}^*_2(2460)^0$ and $D^*_2(2460)^+$ mesons are visible in these plots. We expect positive interference between the neutral $D^0\bar{D}^*_2(2460)^0$ and the charged $D^-D^*_2(2460)^+$ decay amplitudes leading to the same $D^0D^-\pi^+$ final state for the decay of $C = -1$ state, and the scatter plot evidently agrees with this expectation. Because of the interference we do not study $D^0\bar{D}^*_2(2460)^0$ and $D^-D^*_2(2460)^+$ final states separately and define the signal interval for the $D\bar{D}^*_2(2460)$ combinations as $|M_{D^-\pi^+} - m_{\bar{D}^*_2(2460)^0}| < 50$ MeV/c^2 or $|M_{D^0\pi^+} - m_{D^*_2(2460)^+}| < 50$ MeV/c^2 ($m_{\bar{D}^*_2(2460)^0} = 2.461$ GeV/c^2, $m_{D^*_2(2460)^+} = 2.459$ GeV/c^2 [16]).

We perform a separate study of $e^+e^- \to D\bar{D}^*_2(2460)$ and $e^+e^- \to D(\bar{D}\pi)_{\rm non\bar{D}^*_2(2460)}$. The $M_{D^0D^-\pi^+}$ spectrum for the $D\bar{D}^*_2(2460)$ signal interval is shown in Fig. 4(a). A clear peak corresponding to $\psi(4415) \to D\bar{D}^*_2(2460)$ decay is evident near the $D\bar{D}^*_2(2460)$ threshold. Assuming $J^P = 2^+$ for $\bar{D}^*_2(2460)$ mesons [16], the signal of $\psi(4415) \to D\bar{D}^*_2(2460)$ should be described by a d-wave relativistic Breit-Wigner (RBW) function. However, to compare mass and width of the obtained $\psi(4415)$ signal with the corresponding $\psi(4415)$ resonance parameters measured in the *inclusive* study [16], we perform a likelihood fit to $M_{D^0D^-\pi^+}$ distribution with the $D\bar{D}^*_2(2460)$ signal parametrized by an s-wave RBW function. The fit

TABLE I. Contributions to the systematic error on the cross sections [%].

Source	$D^0D^-\pi^+$
Background subtraction	± 5
Cross section calculation	± 5
$\mathcal{B}(D)$	± 4
Reconstruction	± 6
Kaon identification	± 2
Total	± 10

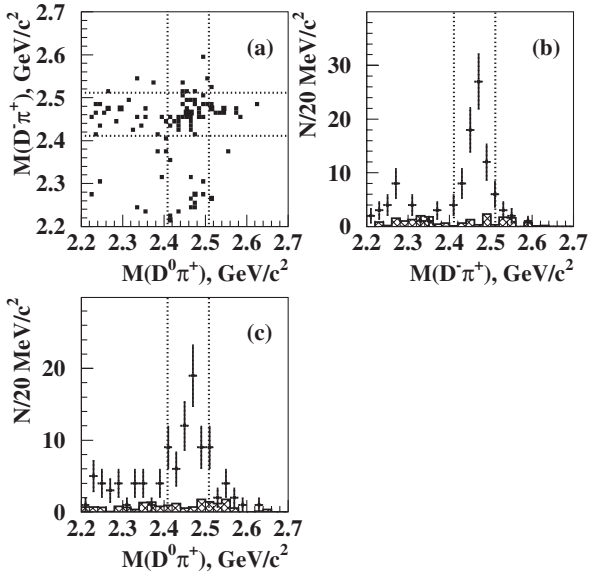

FIG. 3. (a) The scatter plot of $D^-\pi^+$ vs $D^0\pi^+$ for the signal region in the data for $|M_{D^0D^-\pi^+} - m_{\psi(4415)}| < 100$ MeV/c^2. (b) $D^-\pi^+$ and (c) $D^0\pi^+$ mass projections. Histograms show the normalized contributions from the M_{D^0} and M_{D^-} sidebands. The selected mass windows are illustrated by vertical and horizontal lines.

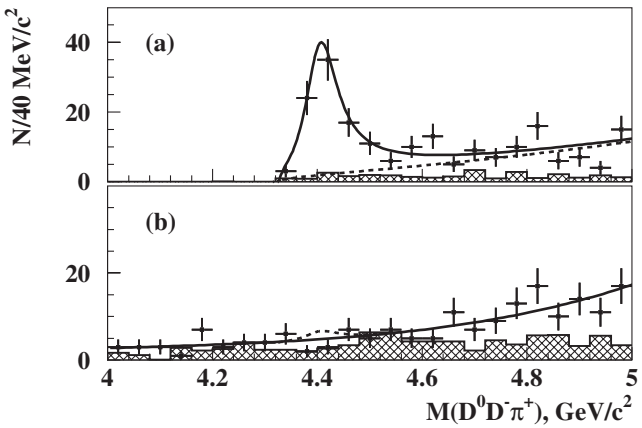

FIG. 4. (a) The $M_{D^0D^-\pi^+}$ spectrum for the $D\bar{D}_2^*(2460)$ signal region. The solid curve represents the result of the fit described in the text. The threshold function is shown by the dashed curve. (b) The $M_{D^0D^-\pi^+}$ spectrum outside the $D\bar{D}_2^*(2460)$ signal region. The solid curve is a fit with a second-order polynomial background function. The dashed curve shows the upper limit on the $\psi(4415)$ yield at 90% C.L. Histograms show the normalized contributions from M_{D^0} and M_{D^-} sidebands.

with the d-wave RBW function, which would be appropriate for the studied decay channel, is found to be unstable with respect to variations in the background parametrization. To account for background and a possible nonresonant $D^0D^-\pi^+$ contribution we use a threshold function $\sqrt{M - m_D - m_{\bar{D}_2^*(2460)}}$ with a floating normalization. Finally, the sum of the signal and background functions is multiplied by the mass-dependent linear efficiency function and differential ISR luminosity. The fit, shown as a solid curve in Fig. 4(a), yields 109 ± 25(stat) signal events. The significance for the signal is obtained from the quantity $-2\ln(\mathcal{L}_0/\mathcal{L}_{\max})$, where $\mathcal{L}_{\max}$ is the maximum likelihood returned by the fit, and $\mathcal{L}_0$ is the likelihood with the amplitude of the Breit-Wigner function set to zero. Taking the reduction in the number of degrees of freedom into account, we determine the significance of the $\psi(4415)$ signal to be $\sim 10\sigma$. The obtained peak mass $m_{\psi(4415)} = (4.411 \pm 0.007(\text{stat}))$ GeV/c^2 and total width $\Gamma_{\text{tot}} = (77 \pm 20(\text{stat}))$ MeV/c^2 are in good agreement with the PDG [16] values, the recent BES results [17] and predictions of Ref. [18]. The peak cross section for $e^+e^- \to \psi(4415) \to D\bar{D}_2^*(2460)$ process at $E_{\text{c.m.}} = m_{\psi(4415)}$ is calculated from the amplitude of the RBW function in the fit to be $\sigma(e^+e^- \to \psi(4415)) \times \mathcal{B}(\psi(4415) \to D\bar{D}_2^*(2460)) \times \mathcal{B}(\bar{D}_2^*(2460) \to D\pi^+) = (0.74 \pm 0.17 \pm 0.08)$ nb. Here the systematic uncertainty is obtained by varying the fit range, histogram bin, and parametrization of the background function and efficiency. Using $\sigma(e^+e^- \to \psi(4415)) = 12\pi/m^2_{\psi(4415)} \times (\Gamma_{ee}/\Gamma_{\text{tot}})$ we calculate the $\mathcal{B}(\psi(4415) \to D\bar{D}_2^*(2460)) \times \mathcal{B}(\bar{D}_2^*(2460) \to D\pi^+) = (10.5 \pm 2.4 \pm 3.8)\%$ using the $\psi(4415)$ parameters from the PDG [16] and $(19.5 \pm 4.5 \pm 9.2)\%$ for the $\psi(4415)$ parameters from Ref. [17].

The shape of the $M_{D^0D^-\pi^+}$ spectrum with the $D\bar{D}_2^*(2460)$ signal excluded, shown as a solid curve in Fig. 4(b), is relatively featureless and, in the $\psi(4415)$ mass window, is consistent with the combinatorial background. The fit to this distribution with the $\psi(4415)$ signal function (an s-wave RBW function with mass and width fixed to the result of the previous fit) and a second-order polynomial function yields a negative $\psi(4415)$ signal that is consistent with zero. We calculate the upper limit on the $\psi(4415)$ yield to be 18 events at 90% C.L. We assume a phase-space-like $\psi(4415) \to D^0D^-\pi^+$ decay and calculate an upper limit on the ratio of the branching fractions of $\psi(4415)$ decays to nonresonant $D^0D^-\pi^+$ and $D\bar{D}_2^*(2460)$. This assumption is not exactly correct since at least one meson pair has to be in a relative p-wave state. However, it provides a conservative estimate of the efficiency of the $D\bar{D}_2^*(2460)$ veto. In this way we obtain $\mathcal{B}(\psi(4415) \to D^0D^-\pi^+_{\text{nonresonant}})/\mathcal{B}(\psi(4415) \to D\bar{D}_2^*(2460) \to D^0D^-\pi^+) < 0.22$ at 90% C.L.

In summary, we report first measurements of the $e^+e^- \to D^0D^-\pi^+$ exclusive cross section over the center-of-mass energy range from 4.0 GeV to 5.0 GeV with initial-state radiation. Aside from a prominent $\psi(4415)$ peak, the c.m. energy dependence of the $e^+e^- \to D^0D^-\pi^+$ cross section has no evident structure. From a study of the resonant structure in $\psi(4415)$ decay we conclude that the $\psi(4415) \to D^0D^-\pi^+$ process is dominated by $\psi(4415) \to D\bar{D}_2^*(2460)$. The mass and width of the $\psi(4415)$ state are

found to be $(4.411 \pm 0.007(\text{stat}))\ \text{GeV}/c^2$ and $(77 \pm 20(\text{stat}))\ \text{MeV}/c^2$, respectively.

We thank the KEKB group for excellent operation of the accelerator, the KEK cryogenics group for efficient solenoid operations, and the KEK computer group and the NII for valuable computing and Super-SINET network support. We acknowledge support from MEXT and JSPS (Japan); ARC and DEST (Australia); NSFC and KIP of CAS (China); DST (India); MOEHRD, KOSEF, and KRF (Korea); KBN (Poland); MES and RFAAE (Russia); ARRS (Slovenia); SNSF (Switzerland); NSC and MOE (Taiwan); and DOE (USA).

[1] J. Siegrist *et al.* (Mark-1 Collaboration), Phys. Rev. Lett. **36**, 700 (1976).
[2] R. Brandelik *et al.* (DASP Collaboration), Phys. Lett. **76B**, 361 (1978).
[3] A. Osterheld *et al.* (Crystal Ball Collaboration), SLAC Report No. SLAC-PUB-4160, 1986.
[4] J. Z. Bai *et al.* (BES Collaboration), Phys. Rev. Lett. **88**, 101802 (2002).
[5] K. K. Seth, Phys. Rev. D **72**, 017501 (2005).
[6] G. Pakhlova, arXiv:0708.0082.
[7] G. Pakhlova *et al.* (Belle Collaboration), Phys. Rev. Lett. **98**, 092001 (2007).
[8] B. Aubert *et al.* (*BABAR* Collaboration), Phys. Rev. Lett. **95**, 142001 (2005).
[9] C. Z. Yuan *et al.* (Belle Collaboration), Phys. Rev. Lett. **99**, 182004 (2007).
[10] X. L. Wang *et al.* (Belle Collaboration), Phys. Rev. Lett. **99**, 142002 (2007).
[11] K. Abe *et al.* (Belle Collaboration), arXiv: 0708.3812 [Phys. Rev. Lett. (to be published)].
[12] A. Abashian *et al.* (Belle Collaboration), Nucl. Instrum. Methods Phys. Res., Sect. A **479**, 117 (2002).
[13] S. Kurokawa and E. Kikutani, Nucl. Instrum. Methods Phys. Res., Sect. A **499**, 1 (2003), and other papers included in this volume.
[14] Charge-conjugate modes are included throughout this Letter.
[15] E. Nakano, Nucl. Instrum. Methods Phys. Res., Sect. A **494**, 402 (2002).
[16] W.-M. Yao *et al.* (Particle Data Group), J. Phys. G **33**, 1 (2006).
[17] M. Ablikim *et al.* (BES Collaboration), arXiv:0705.4500.
[18] T. Barnes, S. Godfrey, and E. S. Swanson, Phys. Rev. D **72**, 054026 (2005).